

Thermodynamic and Transport Properties of Superconducting $Mg^{10}B_2$

D. K. Finnemore, J. E. Ostenson, S. L. Bud'ko, G. Lapertot,* P. C. Canfield
Ames Laboratory, U.S. Department of Energy and Department of Physics and Astronomy
Iowa State University, Ames, Iowa 50011
(April 26, 2024)

Transport and thermodynamic properties of a sintered pellet of the newly discovered MgB_2 superconductor have been measured to determine the characteristic critical magnetic fields and critical current densities. Both resistive transition and magnetization data give similar values of the upper critical field, H_{c2} , with magnetization data giving $dH_{c2}/dT = 0.44 T/K$ at the transition temperature of $T_c = 40.2 K$. Close to the transition temperature, magnetization curves are thermodynamically reversible, but at low temperatures the trapped flux can be on the order of one Tesla. The value of dH_c/dT at T_c is estimated to be about $12 mT/K$, a value similar to classical superconductors like Sn. Hence, the Ginsburg-Landau parameter $\kappa \sim 26$. Estimates of the critical supercurrent density, J_c , using hysteresis loops and the Bean model give critical current densities on the order of $10^5 A/cm^2$. Hence the supercurrent coupling through the grain boundaries is comparable to intermetallics like Nb_3Sn .

74.25.Bt, 74.25.Fy, 74.25.Ha, 74.60.Ge, 74.60.Jg

I. INTRODUCTION

With the discovery of superconductivity in MgB_2 at about $39 K$ by Akimitsu and co-workers,¹ there is an opportunity to study superfluid transport and phase locking of conduction electrons in a whole new class of materials. In early studies of the B isotope effect,² Bud'ko and co-workers found the superconducting transition temperature, T_c , increased from $39.2 K$ for $Mg^{11}B_2$ to $40.2 K$ for $Mg^{10}B_2$ giving a partial isotope exponent $\alpha_B = 0.26$ for the isotope relation $T_c \sim M^{-\alpha_B}$ where M is the isotope mass. This is a clear indication that the phonons are playing an important role in the superconducting interaction. In addition, band structure calculations³ indicate a rather isotropic electrical transport in spite of the very layered appearance of honeycombed boron and hexagonal magnesium networks in the material.

The purpose of this letter is to report measurements of the critical fields of this material to get an estimate of the characteristic length and energy scales for comparison with the classical superconductors like Nb and the high temperature superconductors, like $YBa_2Cu_3O_{7-\delta}$. A second goal is to obtain some measure of the supercurrent transport through grain boundaries for comparison with the high temperature superconductors where there are serious weak link problems with the grain boundaries.

II. EXPERIMENT

A sintered pellet of $Mg^{10}B_2$ was made by sealing a stoichiometric mixture of Mg and ^{10}B in a Ta tube and heating to $950^\circ C$ for two hours.² Magnetization was measured with a Quantum Designs SQUID magnetometer with a $60 mm$ scan length on a $14.22 mg$ piece from the same batch of $Mg^{10}B_2$ material reported previously.² Electrical resistance between $1.9 K$ and $300 K$ in applied magnetic field up to $9 T$ was measured in a Quantum Designs PPMS-9 apparatus on another piece from the same $Mg^{10}B_2$ batch using standard four probe ac resistance technique at $f = 16 Hz$ and a current density of $0.1 - 0.3 A/cm^2$. Electrical contacts were made with Epo-tek $H20E$ silver epoxy.

III. RESULTS AND DISCUSSION

The temperature dependent electrical resistance of the material from $300 K$ to $1.9 K$, shown in Fig. 1, roughly obeys $R = R_0 + R_1 T^3$ power law in the normal state. The residual resistance ratio (RRR) is approximately 20, which is relatively high for a sintered polycrystalline sample. Near T_c , the data show considerable flux-flow broadening as shown by the inset in Fig. 1 where the scans range from 0 to $9 T$. Transition widths gradually broaden from $0.5 K$ at 0 field to $9.5 K$ at $\mu_0 H = 9 T$ indicating a broad region of flux-flow resistivity.⁴ The extent of this flux-flow regime is delineated by the onset and completion temperatures shown in Fig. 2 by the vertical dash lines.

Possibly the most interesting aspect of these data is the strong magnetoresistance which shows the resistance at $45 K$ rising approximately 80 percent in $9 T$. If these data are plotted on a Kohler Plot shown in Fig. 3, the $\Delta\rho/\rho_0$ vs. H/ρ_0 curve is a straight line for the change of temperature at constant field (open circles) and for changing field at constant temperature (solid triangles). This observation is consistent with the observed magnetoresistance being a band effect and intrinsic to the sample.

Magnetization data are exemplified by the $36 K$ and $30 K$ runs in Fig.4. For the $30 K$ run, the magnetization abruptly departs from the background at $H_{c2} = 4.4 T$ and is reversible to an accuracy of one percent of the magnetization down to $H_{irr} = 1.6 T$. Because the background magnetization is very small, linear in magnetic field, and independent of temperature between $42 K$ and

50 K, this correction is easily made and H_{c2} and H_{irr} are fairly easy to measure. At 7 T, the magnitude of the background is about 0.13 emu/cm^3 and the correction can be made to an accuracy of 0.01 emu/cm^3 . The inset shows that the irreversible magnetization over a fuller temperature range. In the inset, the x-symbols show the 30 K data and show that about 200 emu/cm^3 or about 0.2 T flux is trapped at zero field. At 6 K, shown by the solid squares of the inset, the trapped flux at zero applied field for this rather porous granular pellet is 500 emu/cm^3 or over 0.5 T .

Using the Bean⁵ model with $J_c = 17\Delta M/r$, the critical current densities of Fig. 5 can be derived. Here, J_c is in A/cm^2 , ΔM in emu/cm^3 , and the sample radius, r , in cm . These J_c values are not as high as a sintered pellet of Nb_3Sn ,⁵ but the grain-to-grain supercurrent coupling is rather promising. A scanning electron microscope picture of a fracture surface of the pellet shows grain size running from about $0.5 \mu\text{m}$ to $5 \mu\text{m}$. The grains are somewhat faceted plates and many small grains are equiaxed. From the magnitude of the measured screening currents, it is clear that the proper r to put in the Bean model is the full sample diameter and not the grain size. The sample radius is about 1 mm .

Close to T_c , there is a reasonable range of thermodynamic reversibility, so an estimate has been made of H_c vs. T . To do this, it is assumed that the flux pinning in decreasing magnetic field is the same as in increasing magnetic field and an equilibrium magnetization is defined as the average of the average of the increasing field magnetization and the decreasing field magnetization by $M_{eq} = (M_{inc} + M_{dec})/2$. Willemin and co-workers⁶ have shown the validity of this procedure. A plot of M_{eq} vs. T in Fig.6 shows behavior close to that predicted by Abrikosov.⁷ Integrating the area under these magnetization curves gives the H_c vs. T curve shown in the inset of Fig. 6. From the slope of $dH_c/dT = 119 \text{ Oe/K}$, one can calculate the jump in specific heat at T_c to be $\Delta C = [VT_c/4\pi][dH_c/dT]^2 = 79 \text{ mJ/mole K}$. This is consistent with the direct specific heat measurements published earlier² from which ΔC can be estimated to be about 84 mJ/mole K .

IV. CONCLUSIONS

The transport and magnetization studies of $Mg^{10}B_2$ give very consistent measures of $H_{c2}(T)$ for this material with magnetization data giving a slope at T_c of $dH_{c2}/dT = 0.44 \text{ T/K}$. The magnetization H_{c2} agrees with the onset of the resistive transition, and the broadened resistive transitions seem to reflect a flux-flow resistivity phenomenon. Close to T_c , the values of the H_c can be estimated and the slope is found to be $dH_c/dT = 0.012\text{T/K}$. This then means that the Ginsburg-Landau parameter, $\kappa = H_{c2}/[.707H_c] \simeq 26$. By estimating $H_{c2}(T = 0) = 0.71T_c[dH_{c2}/dT]_{T_c}$ to be 12.5 T , the low

temperature coherence distance, $\xi_o = [\phi_o/[2\pi H_{c2}]]^{1/2}$ is found to be 5.2 nm . Using the relation $\kappa = \xi_o/\lambda$, the penetration depth, $\lambda = 140 \text{ nm}$.

The critical current densities for this rather porous sintered sample are on the order of 10^5 A/cm^2 at 6 K . This would seem to indicate that MgB_2 grain boundaries can transmit rather large supercurrents.

V. ACKNOWLEDGMENTS

We would like to thank M. J. Kramer and F. Laabs for the electron microscope pictures, and V. G. Kogan for useful discussions. C. Petrovic and C. E. Cunningham also made valuable contributions. Ames Laboratory is operated for the U. S. Department of Energy by Iowa State University under contract No. W-7405-ENG-82 and supported by the DOE, the Office of Basic Energy Sciences.

*On leave from Commissariat a l'Energie Atomique, DRFMC-SPSMS, 38054 Grenoble, France.

-
- ¹ J. Akimiitsu, Symposium on Transition Metal Oxides, Sendai, January 10, 2001; J. Nagamatsu, N. Nakagawa, T. Muranaka, Y. Zenitani, and J. Akimitsu (to be published).
 - ² S. L. Bud'ko, G. Lapertot, C. Petrovic, C. Cunningham, N. Anderson, and P. C. Canfield, Phys. Rev. Lett. (in press).
 - ³ J. Kortus, I. I. Mazin, K. D. Belashchenko, V. P. Antropov, and L. L. Boyer, cond-mat/0101446.
 - ⁴ Y. B. Kim and M. J. Stevens, Superconductivity, Ed. R. D. Parks, 1969, Marcel Dekker, Inc, New York, p 1149.
 - ⁵ C. P. Bean, Phys. Rev. Lett. **8**, 225 (1962).
 - ⁶ M. Willemin, C. Rossel, J. Hofer, H. Keller, A. Erb, and E. Walker, Phys. Rev. **58**, R5940 (1998).
 - ⁷ A. A. Abrikosov, Zh. Eksp. Teor. Fiz. 32, 1442 (1957) [Sov. Phys. JETP **5**, 1174 (1957)].

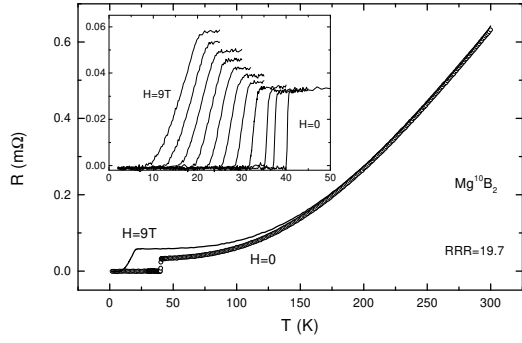


FIG. 1. Resistance of $Mg^{10}B_2$ sample in zero and in 9 T applied field. Inset: resistive superconducting transition in different applied fields (right to left): 0 T, 0.5 T, and from 1 T to 9 T in steps of 1 T.

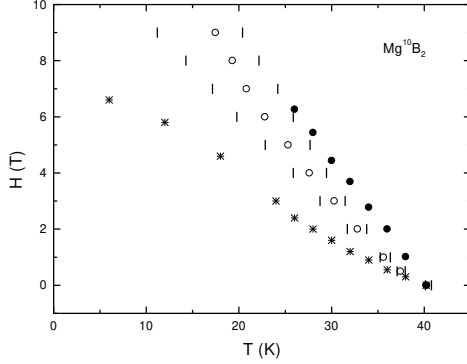


FIG. 2. Upper critical field of $Mg^{10}B_2$ determined resistively (onset and offset are vertical bars and maximum slope points are the open circles) and from magnetization (filled circles). Asterisks show H_{irr} .

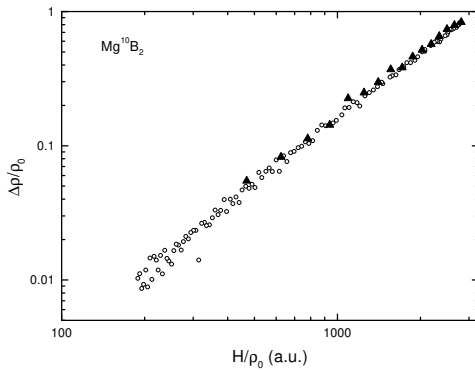


FIG. 3. Kohler plot for $Mg^{10}B_2$: open circles from temperature-dependent resistance from 0 T to 9 T and filled triangles from field-dependent resistance at 45 K.

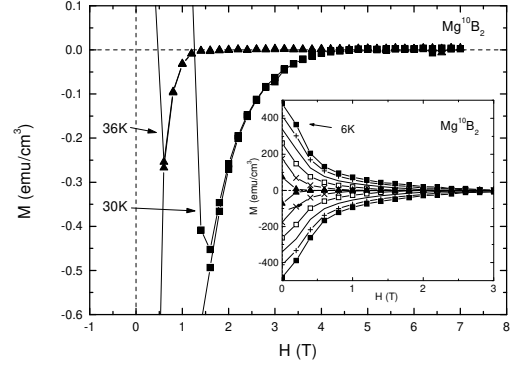


FIG. 4. Expanded view of magnetization vs. field to show the reversible range and the H_{irr} region. Inset shows the full range of magnetization up to 4 T.

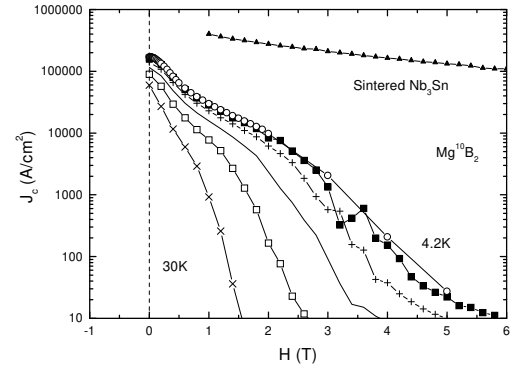


FIG. 5. Comparison of $J_c(H, T)$ up to 30 K with published data for a sintered Nb_3Sn sample at 4.2 K.

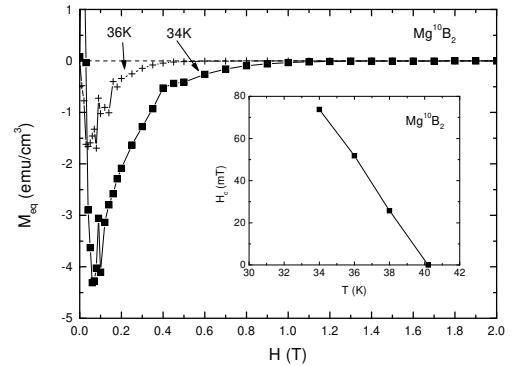


FIG. 6. $M_{eq} = (M_{inc} + M_{dec})/2$ vs. T plot to show the extension of the reversible magnetization into the irreversible range assuming that flux pinning is the same for increasing and decreasing fields. The inset shows the resulting values of H_c .